

WARLEY HUDSON CAMPOS

INDUCTION AND REVERSION OF MAGNETIC
MONOPOLE IN CONCAVE SURFACES OF TOPOLOGICAL
INSULATORS

Dissertation submitted to the Department of
Physics of Universidade Federal de Viçosa, in
partial fulfillment of the requirements of the
Graduate Program in Physics, for the title of
Magister Scientiae.

VIÇOSA
MINAS GERAIS - BRASIL

2016

**Ficha catalográfica preparada pela Biblioteca Central da
Universidade Federal de Viçosa - Câmpus Viçosa**

T

C198i
2016 Campos, Warley Hudson, 1992-
Induction and reversion of magnetic monopole in
concave surfaces of topological insulators / Warley Hudson
Campos. - Viçosa, MG, 2016.
x, 39f. : il. (algumas color.) ; 29 cm.

Inclui apêndice.

Orientador : Winder Alexander de Moura-Melo.

Dissertação (mestrado) - Universidade Federal de
Viçosa.

Referências bibliográficas: f.36-39.

1. Monopolo magnético. 2. Superfícies (Física) -
Propriedades magnéticas. I. Universidade Federal de Viçosa.
Departamento de Física. Programa de Pós-graduação em
Física Aplicada. II. Título.

CDD 22. ed. 538.3

WARLEY HUDSON CAMPOS

INDUCTION AND REVERSION OF MAGNETIC
MONOPOLE IN CONCAVE SURFACES OF TOPOLOGICAL
INSULATORS

Dissertation submitted to the Department of
Physics of Universidade Federal de Viçosa, in
partial fulfillment of the requirements of the
Graduate Program in Physics, for the title of
Magister Scientiae.

APPROVED: July 13, 2016.

Winder A. Moura-Melo
(Adviser)

Jakson Miranda Fonseca
(Co-Adviser)

José Arnaldo Redinz

Joaquim Bonfim Santos Mendes

Acknowledgements

I take this opportunity to thank and dedicate this dissertation to my parents, Vantuir and Amélia, who had a difficult and humble youth, and didn't have the opportunity to study. Nevertheless, they recognized how important studies are for me, and even not understanding my choice of profession, they made all the possible so I could do what I like. I thank them for believing in me, even when I didn't believe in myself, which gave me the will to go ahead. I thank my brother Wallyson for his fellowship in life, showing himself a great friend in the last years. My grandmother, Nair, for being the kindest person alive, always doing what she can to please everyone and specially her grandchildren. To the friends I made in Viçosa, being my second family, which helped, entertained, and encouraged me when I needed. I am really grateful to my girlfriend Bruna, who has been always by my side, supporting and celebrating with me all these years. Having you to help me in this journey was vital and made all difference in my life.

I couldn't forget to thank the department of physics of the Federal University of Viçosa, including all the staff, for being attentive and helpful, making this place very pleasant to be there. To my advisor Winder and my co-advisor Jakson, for the fruitful discussions and advices not only about physics, but also about important decisions on my professional life.

Thanks for the CAPES agency, that has supported me financially, without which I could never go on with my studies.

Contents

List of Figures	v
Resumo	ix
Abstract	x
1 Introduction	1
1.1 Condensed Matter Physics	1
1.2 Landau theory of condensed matter	2
1.2.1 Fermi liquids	2
1.2.2 Phase transitions	2
1.3 Quantum Hall (QH) state	3
1.4 Topological Invariants	6
2 Topological Insulators	8
2.1 Bi-dimensional topological insulators	8
2.1.1 General properties	9
2.1.2 Fractional charge and quantized current	11
2.1.3 Spin-charge separation	12
2.2 Three-dimensional topological insulators	14
2.2.1 General properties	14
2.2.2 Surface quantum Hall effect	15
2.2.3 Majorana fermions on topological insulators	16
3 Topological magneto-electric effect (TMEE)	17
3.1 A different way of inducing electric polarization and magnetization	17
3.2 Deflection of light by the surface of a topological insulator	20
3.2.1 Faraday effect	20

3.2.2	Kerr effect	21
3.3	Magnetic monopoles (and dyons)	22
4	Semi-spherical topological insulator	27
4.1	TMEE on the semi-spherical TI surface	27
4.2	Magnetic field analysis and image magnetic charge configuration	29
4.3	Conclusions and Prospects	34
4.4	Appendix	35
	References	36

List of Figures

1.1	Breaking the continuous rotational symmetry of water by freezing it into a snowflake, which presents a six-fold symmetry. An order parameter ψ develops once the temperature drops below the transition temperature T_c (Source: Ref. [2]).	3
1.2	The Hall conductivity does not change smoothly with the variation of the external magnetic field, but is quantized in integer multiples of $\frac{e^2}{h}$. (Source: http://blog510-eslfb.blogspot.com.br/2012/09/efeito-hall-quantico-novo-paradigma-da.html).	4
1.3	Schematic illustration of the Quantum Hall state, and its band structure with a metallic edge state inside the bulk energy gap [7].	5
1.4	Electrons at the metallic bound states naturally avoid non-magnetic impurities, leading to an electric current with no dissipation at the edges of the sample	5
1.5	A circle can be smoothly deformed into a triangle or square, keeping the number of holes a topological invariant.	6
1.6	A circle can not be smoothly deformed into an “infinity” symbol, and vice versa, since it would be necessary to “rip” it in order to make such transformation.	6
1.7	A cup of coffee is topologically equivalent to a “donut” (torus), since both of them have the same amount of holes (genus=1) and can be deformed one to another [1]. (Source: http://www.rikenresearch.riken.jp/images/figures/hi_4626.jpg)	7
2.1	2-D topological insulators have gapped structure band at the bulk, but edge metallic states which lies inside the bulk insulating gap. Electrons with anti-parallel spins propagate at opposite directions, due to the time reversal symmetry. (Source: Ref. [7])	9

2.2	a) Destructive interference of light beams in antireflection lens. b) There are two possible paths for electrons to be backscattered by a nonmagnetic impurity, but these paths have a phase difference of π at their wavefunctions, which leads to a destructive interference of the two paths. Source: [8]	10
2.3	a) In conventional materials, 2 movement directions and 2 spin orientations (4 degrees of freedom) are present for each electron. b) Helical edge states present only two degrees of freedom due to the spin-momentum locking. . . .	11
2.4	A) If the domain wall is anti-phase, it carries half of the electronic charge. The blue arrows show the magnetic domain wall configuration and the red curve shows the charge density distribution. B) A rotation in the magnetic field where θ goes from 0 to 2π induces the pump of a quantized charge e through the 1-D system. The blue circle with arrow shows the magnetic field rotation trajectory. (Source: [15])	12
2.5	There are four different types of fluxons. The notation, e.g., $f_{+(1/2)\uparrow,-(1/2)\downarrow}$, means that the spin-up zero mode is filled while spin-down zero mode is empty. (Source: Ref. [17]).	13
2.6	The a) charge and b) spin densities of a pair of fluxons on a 24×24 lattice with periodic boundary condition. The fluxon at coordinate (6, 6) is $f_{+(1/2)\uparrow,+(1/2)\downarrow}$, it has charge 1 and $S_z = 0$. The fluxon at (18,18) is $f_{+(1/2)\uparrow,-(1/2)\downarrow}$, it has charge 0 and $S_z = 1/2$. The figure illustrates the spin-charge separation in real space. (Source: Ref. [17])	13
2.7	Electrons in a 3-D topological insulator are allowed to move in any direction along the surface, but its spin orientation (red) is related to its direction of motion (blue), in such a way that they are always perpendicular to each other and both tangent to the surface. (Source: Ref. [7]).	14
2.8	Quantum Hall effect on the surface of a topological insulator. a) An external magnetic field breaks the time reversal symmetry and gives rise to Landau levels. b) Top and bottom surfaces share a single chiral edge state, which has net integer quantized Hall conductivity. c) A thin magnetic insulator film induces an energy gap at the surface spectrum. d) A domain wall in the surface magnetization exhibits a chiral fermion mode. (Source: Ref. [6]). . .	16

3.1	The TMEE manifests with electromagnetic topological responses that are independent on details of the system. a) Application of an external electric field induces a topological magnetization response. b) Application of an external magnetic field induces a topological electric polarization response. Source: (Ref. [13])	19
3.2	Illustration of the Faraday effect on the surface of a topological insulator, the transmitted light suffers a rotation of θ_F at its plane of polarization. (Source: Ref. [13])	21
3.3	Electric charge near the plane interface between a topologically trivial insulator and a three-dimensional topological insulator. The electric field of the point-like charge induces the usual polarization at the topological insulator plus a surface quantized Hall current. This current generates a magnetic field that can be described by image magnetic monopoles. The red lines represent the electric field, the blue lines represent the magnetic field and the circulating black lines represent the surface Hall current. (Source: Ref. [26]).	23
3.4	Illustration of an experimental apparatus that can be used to measure the magnetic field distribution generated by an image magnetic monopole, next to the surface of a topological insulator. (Source: Ref. [26])	25
4.1	Illustration of magnetic monopoles charge reversion as the point-like electric charge crosses the semi-sphere focus. In figure a), $z_0 > 0$, so the Hall current is always clockwise (see inset), which indicates a negative image magnetic monopole. In figure b), $z_0 < 0$, so the Hall current is counter-clockwise, and the monopole has positive magnetic charge (see inset). Notice that in figure a), the tangential components of the electric field point radially inwards, what never happens in positively curved surfaces. The red lines represent the electric field and the black circles represent the circulating surface current \mathbf{J} . The magnetic field lines were omitted for simplicity. z_0 is the position of the electric charge q , relative to the origin of the coordinate system. μ_1 and ϵ_1 (μ_2 and ϵ_2) are the magnetic permeability and the dielectric constant of the conventional insulator (topological insulator), respectively.	28

4.2	Behaviour of the magnetic field along the z -axis, generated by the Hall current on the semi-spheric interface. It is shown for different values of z_0 , evidencing the change in the field's sign when the electric charge crosses the semi-sphere focus ($z = 0$). Intersection of the z -axis with the surface occurs at $z = -1$, since $R = 1$. In the vertical axis label, c is the speed of light.	29
4.3	The electric charge is brought near the surface, and the magnetic field approaches to the one of an image point-like magnetic charge.	30
4.4	Comparison between the magnetic fields generated by the Hall current and by the image magnetic monopole g_1 near the reverse point. We consider the electric charge very close to the surface ($z_0 = -0.95$). The fields are shown in the same region as the electric charge, while the monopole is located inside the topological insulator. If the magnetic monopole is exactly in the reverse point, the concordance between the Hall current's magnetic field and the magnetic monopole's field is perfect.	31
4.5	Comparison between $\ln B$ for both the fields generated by the Hall current and by the magnetic monopole. The electric charge is located close to the surface of the topological insulator ($z_0 = -0.95$). Note that when looking far away from the surface, the fields mismatches.	32
4.6	Variation of the magnetic monopole intensity with the distance between the electric charge and the TI surface. Notice that g_1 grows linearly with the distance in the region where the magnetic monopole picture is valid.	33
4.7	Comparison between the real magnetic field, generated by the Hall current on surface, and the fields of the image monopoles, when the electric charge is not close to the surface, but still inside the concavity ($z_0 = -0.4$). In this situation, the field generated by the lines of magnetic charge density are not negligible, so the curves in the graph do not fit very well, since we are taking in account only the field generated by the magnetic monopole.	33

Resumo

CAMPOS, Warley Hudson, M.Sc, Universidade Federal de Viçosa, julho de 2016. **Indução e reversão de monopolo magnético em superfícies côncavas de isolantes topológicos.** Orientador: Winder Alexander de Moura Melo. Coorientadores: Jakson Miranda Fonseca, Afrânio Rodrigues Pereira e Clodoaldo Irineu Levar-toski de Araujo.

Nesta dissertação nós investigamos uma nova classe de materiais, recentemente descoberta, que possui propriedades intrigantes com perspectivas substanciais de aplicações tecnológicas. Esses são os chamados isolantes topológicos (IT's), uma vez que são isolantes no “bulk” mas com funções de onda associadas carregando topologia não-trivial, o que proporciona estados de condução nas bordas protegidos por simetria de reversão temporal (SRT). Esses estados se propagam em sentidos opostos de acordo com seu spin, o que abre uma janela interessante para aplicações tecnológicas, tais como computação quântica e “spintrônica”.

Ao revestir a superfície de um IT 3-D com um filme ferromagnético, quebra-se a SRT e é criado um gap nos estados de borda. Esse gap dá origem a uma condutividade Hall quantizada em valores semi-inteiros, levando ao efeito magneto-elétrico topológico (EMET), que consiste de uma resposta tanto elétrica quanto magnética do material devido a um campo externo, seja ele elétrico ou magnético.

Sabe-se que uma carga elétrica perto da superfície de um isolante topológico induz um monopolo magnético imagem em seu interior (“bulk”), devido ao EMET. Calculamos o campo magnético resultante de uma configuração específica, quando a superfície topológica tem uma curvatura negativa, particularmente no caso de uma concavidade semi-esférica. Analisando o campo magnético, mostramos que o monopolo magnético imagem inverte seu sinal quando a carga elétrica atravessa o foco da semi-esfera. Além disso, existe uma linha de densidade de carga magnética na configuração de cargas imagem, que também inverte seu sinal. Essas reversões são características de superfícies com curvatura negativa, e não acontecem em IT's perfeitamente esféricos ou planos. Quando a carga elétrica é trazida para perto da superfície, o campo magnético local se comporta como o de um monopolo magnético sozinho, como esperado, uma vez que localmente temos uma superfície plana.

Abstract

CAMPOS, Warley Hudson, M.Sc, Universidade Federal de Viçosa, July, 2016. **Induction and reversion of magnetic monopole in concave surfaces of topological insulators.** Adviser: Winder Alexander de Moura Melo. Co-Advisers: Jakson Miranda Fonseca, Afrânio Rodrigues Pereira and Clodoaldo Irineu Levartoski de Araujo.

In this dissertation we have investigated a new class of materials, recently discovered, that has intriguing properties with substantial prospects of technological applications. These are the so-called topological insulators (TI's), once their bulks are insulating but with associated wavefunctions carrying non-trivial topology, what provides conducting states at their edges protected by time reversal symmetry (TRS). These states are counter propagating relative to their spin, which opens an interesting window for technological applications, such as quantum computation and “spintronics”.

By coating the surface of a 3-D TI with a ferromagnetic film, one breaks the TR symmetry and creates a gap in the edge states. This gap gives rise to a half-integer quantized Hall conductivity, leading to the topological magneto-electric effect (TMEE), which consists of both an electric and magnetic response of the material due to an external field, whether electric or magnetic.

It is known that an electric charge near the surface of a topological insulator induces an image magnetic monopole inside its bulk, due to the TMEE. We have calculated the magnetic field resulting from a specific configuration, when the topological surface has a negative curvature, particularly in the case of a semi-spherical concavity. Analysing the magnetic field, we show that the image magnetic monopole reverses its sign when the electric charge crosses the focus of the semi-sphere. In addition, there is a line of magnetic charge density in the image charge configuration, which also reverses its sign. These reversions are characteristic features of negative curved surfaces, and cannot happen in perfectly spherical or plane TI's. When the electric charge is brought near the surface, the local magnetic field then recovers that due to a magnetic monopole alone, as expected, since locally we have a plane surface.

Chapter 1

Introduction

1.1 Condensed Matter Physics

Since the beginning of XX century, quantum mechanics has shown itself a powerful tool to study systems of individual or small groups of particles. Many properties of atoms and molecules can be explained from the orbital atomic model. But when dealing systems with the number of particles in the order of 10^{23} , Schrödinger's equation is intractable mathematically, and it was necessary a new branch of physics devoted to study this kind of system, which is called Condensed Matter Physics.

When a great number of particles are brought together, they tend to reorganize themselves in order to establish a state of matter, which can be gas, solid, liquid, or many others, being able even to switch between some of these states under certain conditions. Despite of being composed by the basic constituents of matter, such as ions and electrons, these states usually have properties quite different from their constituents, having their own elementary excitations and presenting, therefore, a new set of physical laws ruling the collective behaviour of the system. An example of elementary excitation would be phonons, which are low-energy excitations caused by collective motion of ions in the lattice of a solid state system. Condensed Matter Physics studies aspects that explain how order emerges in such systems and how their constituents interact to each other[1].

Facing these phenomena, a theory was developed to study the condensates of matter that arises from interactions between atoms. The Landau paradigms were able to explain all states of matter (insulators, conductors, superconductors, etc.) known until most of 20th century, and consists of two theories, which are the scope of the next

section.

1.2 Landau theory of condensed matter

1.2.1 Fermi liquids

The non-interacting Fermi gas model is widely used to portray the metallic behaviour of some materials, and reproduces many of its qualitative features, such as a well-defined Fermi surface, a linear specific heat capacity, and a temperature-independent paramagnetic susceptibility. However, in metals at low temperatures, the Coulomb energy is comparable to the electrons kinetic energy, constituting a major perturbation to the electrons motions. The Landau-Fermi liquids theory allows to continue using the idea of independent particles, even in the presence of strong interactions, due to the concept of quasi-particles. A quasi-particle is the adiabatic evolution of the non-interacting into an interacting fermion environment. In this process, the conserved quantum numbers such as charge, spin and momentum are unchanged, but its dynamical properties, the effective magnetic moment and mass of the quasi-particle are “renormalized” to new values g^* and m^* , respectively. Thus, there is a one-to-one correspondence between the elementary excitations of a Fermi gas system and a Fermi liquid system [2, 3].

1.2.2 Phase transitions

The phase transitions theory relates the phases of matter with the different symmetries in each phase, wherein a change in the symmetry of material corresponds to a change in its phase. Such transitions can be better understood using the concept of order parameter, introduced by Landau, as a means to quantify the dramatic transformation of matter at a phase transition. This order parameter ψ develops in a phase transition once the temperature drops below the critical temperature T_c :

$$|\psi| = \begin{cases} 0 & (T > T_c) \\ |\psi_0| > 0 & (T < T_c) \end{cases} \quad (1.1)$$

The emergence of an order parameter indicates a break in the symmetry and affects drastically the macroscopic properties of the material. For instance, water droplets are perfectly spherical when subjected to zero gravity, but if cooled through their freezing point, they form crystals of water with the six-fold symmetry of a snowflake (Fig. 1.1).

We say that the symmetry of water was spontaneously broken, because the ice crystal no longer enjoys the continuous rotational symmetry of the original water droplet. Other common examples are the alignment of spins in a ferromagnetic material, and the emergence of superconductivity and superfluidity phases due to the cooling of quantum fluids [2].

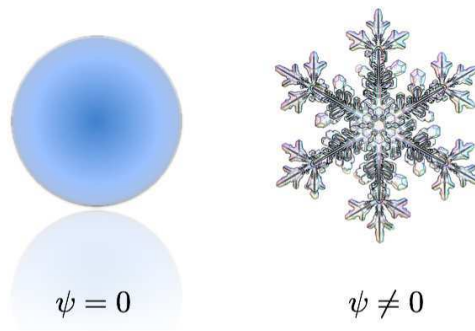


Figure 1.1: Breaking the continuous rotational symmetry of water by freezing it into a snowflake, which presents a six-fold symmetry. An order parameter ψ develops once the temperature drops below the transition temperature T_c (Source: Ref. [2]).

The Landau order parameters vary continually and differentiably in function of external parameters (temperature, magnetic field, etc.), except in critical points, where the symmetry is broken, and the phase transition takes place. This is a characteristic feature of this non-topological theory, and a crucial point to understand the importance of the remarkable state of matter described in the next section.

1.3 Quantum Hall (QH) state

In the year of 1980, Klaus von Klitzing was studying the Hall conductance of a two-dimensional electron gas at very low temperatures, at the Grenoble High Magnetic Field Laboratory, in France [4]. He discovered that the Hall conductance (conductivity in a direction perpendicular to an applied electric field) exhibits a staircase sequence of wide plateaus as a function of the magnetic field (Fig. 1.2), applied normal to the gas plane. With high precision, the successive values of the Hall conductance were integer multiples of e^2/h , where e is the electronic charge, and h is the Plank constant [5].

We can understand this state in a simplified way by considering the movement

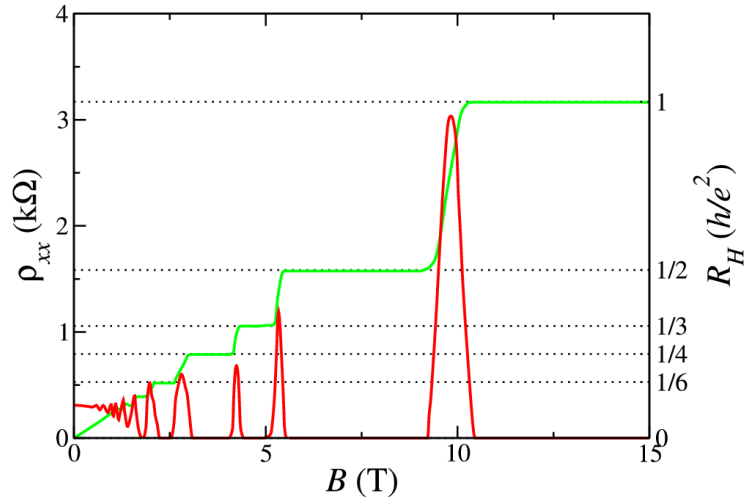


Figure 1.2: The Hall conductivity does not change smoothly with the variation of the external magnetic field, but is quantized in integer multiples of $\frac{e^2}{h}$. (Source: <http://blog510-eslfb.blogspot.com.br/2012/09/efeito-hall-quantico-novo-paradigma-da.html>).

of the electrons along the bi-dimensional gas (Fig. 1.3). They can be considered nearly free so that the ions do not take place at interactions, but the application of a perpendicular magnetic field makes the carriers to move in cyclotron orbits. Their quantization with cyclotron frequency ω_c leads to quantized Landau levels with energy $\epsilon_m = \hbar\omega_c(m + 1/2)$. If N Landau levels are filled and the rest are empty, then an energy gap separates the occupied and empty states just as in an insulator. Unlike an insulator, though, an electric field causes the cyclotron orbits to drift, leading to a Hall current characterized by the quantized Hall conductivity [6]:

$$\sigma_{xy} = Ne^2/h, \quad (1.2)$$

where N is an integer.

Landau levels can be viewed as a “band structure”, where the bulk of the material presents gaps, as in an insulator. At the boundaries, instead, the carriers are unable to perform a closed orbit, and propagate along the material in directionally defined metallic states (Fig. 1.3). The metallic states are different from the ordinary states of matter because they persists even in the presence of impurity and do not vanish as in an usual conductor. The electronic states responsible for this motion are *chiral* in the sense that they propagate in only one direction along each edge. These states are insensitive to disorder because there are no states available for backscattering, a

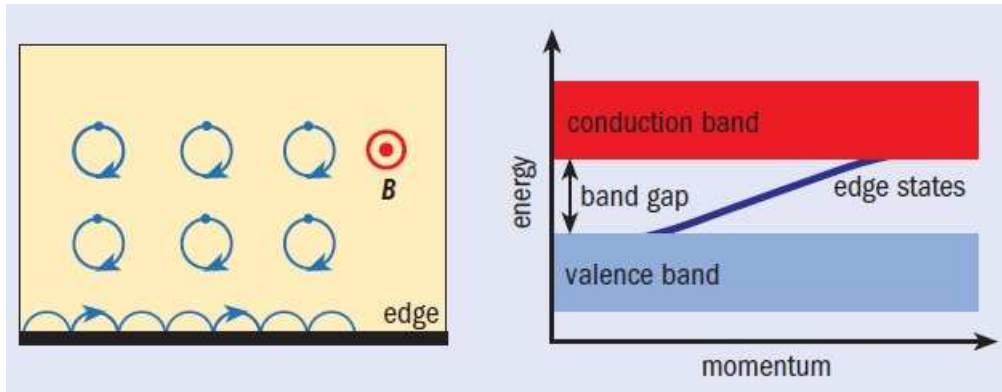


Figure 1.3: Schematic illustration of the Quantum Hall state, and its band structure with a metallic edge state inside the bulk energy gap [7].

fact that underlies the perfectly quantized electronic transport in the quantum Hall effect [6]. This absence of scattering is reflected macroscopically as currents with no dissipation, since the electrons avoid non-magnetic impurities naturally (Fig. 1.4), which is a really interesting potential for technological applications.

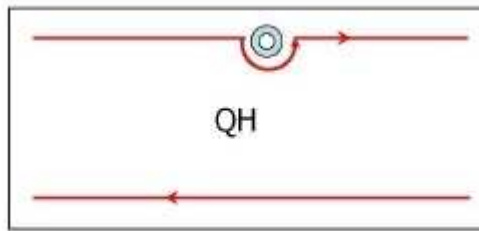


Figure 1.4: Electrons at the metallic bound states naturally avoid non-magnetic impurities, leading to an electric current with no dissipation at the edges of the sample

Hall conductance is the order parameter that characterizes this state of matter, which can not be described by Landau theory, because there is no symmetry being spontaneously broken in the emergence of this order parameter. Its behaviour depends only on its topology and not on its specific geometry; it is topologically distinct from all previously known states of matter [8]. Differently of the states described by Landau's paradigms, at the QH state the order parameter does not smoothly changes with the variation of the external magnetic field, but it topologically quantized. Small variations at the magnetic field keep the Hall conductivity unchanged (Fig. 1.2). We say that this state has **topological order**. The topological order “protects” the edge states so that they can not be easily eliminated due to damages at the surface by chemical or

mechanical means, changing its shape or orientation in relation to the crystal lattice (since these changes are applied moderately) [9].

1.4 Topological Invariants

Topology is an area of mathematics that studies the properties of objects that are topologically invariant under smoothly deformations. A circle, by instance, can be smoothly deformed into a triangle or in a square without the necessity of “rip” or “stick” it (Fig. 1.5). This happens because all these geometric shapes have only one “hole” in their figures, we say therefore that the number of holes is a topological invariant under such transformations.

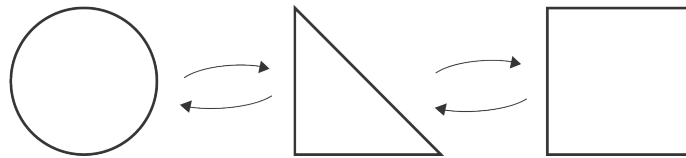


Figure 1.5: A circle can be smoothly deformed into a triangle or square, keeping the number of holes a topological invariant.

A presumed counter-example would be that of a circle being deformed into an “infinity” symbol, however this is not a smooth transformation, since it would be necessary to “rip” the circle in order to transform it. (Fig. 1.6)

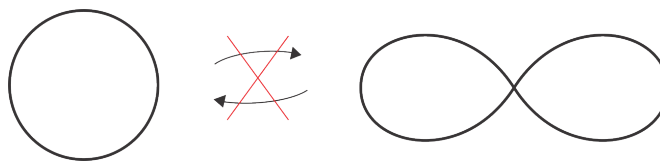


Figure 1.6: A circle can not be smoothly deformed into an “infinity” symbol, and vice versa, since it would be necessary to “rip” it in order to make such transformation.

In 3-D, the Gauss-Bonnet theorem guarantee that the surface integral of the Gauss curvature (κ) over the object depends only on the amount of holes g (genus):

$$\int_S \kappa dS = 2\pi(2 - g) \quad (1.3)$$

A classical example consists of a “donut” which can be smoothly transformed into a cup of coffee (Fig. 1.7)[10], where $g = 1$ in both three-dimensional objects. In

a mathematical point of view, the topological classification focuses on fundamental distinctions between the shapes and discards small details [1].



Figure 1.7: A cup of coffee is topologically equivalent to a “donut” (torus), since both of them have the same amount of holes (genus=1) and can be deformed one to another [1]. (Source: http://www.rikenresearch.riken.jp/images/figures/hi_4626.jpg)

In the context of topological states of matter, such smooth deformation consists in an adiabatic change in the Hamiltonian that does not “closes” the energy gap. In the sense that the perturbation does not do that the valence and conduction bands touch each other, either with addition of impurities or deformations at the material.

Chapter 2

Topological Insulators

The topological states of matter are characterized by order parameters which are topologically invariant. Since the discovery of topological order with the quantum Hall state, new states of matter with topological order have been enthusiastically searched. The only topological state of matter known until 2005 was the quantum Hall state, but in 2006 a topological order in bi-dimensional HgTe quantum wells was proposed by *Bernevig et al.* [11], and experimentally observed in the following year by *König et al.* [12]. This state of matter was named the quantum spin Hall (QSH) state, due to the helical electronic states it presents, and constitutes what we call a bi-dimensional topological insulator. Since then, TI's have caused a great impact in the scientific community due to their intriguing properties and prospectives of technological applications [7]. The possibility of produce spin currents using these materials makes the topological insulators a great potential for applications in spintronics (similar to electronic, but in this case the electronic spins also carry information).

2.1 Bi-dimensional topological insulators

The quantum spin Hall state differs from the quantum Hall mainly because of their physical origin. The latter requires a high external magnetic field to exist, which is a great limitation for practical applications. Furthermore, the magnetic field breaks the time-reversal symmetry, and by changing the electronic movement (applying the time reversal operator), we modify the state of the system. The QSH state, otherwise, has its properties originated from its electronic structure, and does not need any external interference to occur.

Topological insulators where discovered in a search for exotic states of matter with

time reversal symmetry. In materials where the QSH effect occurs, interaction between the electronic spins and the magnetic field created by the atoms (spin-orbit interaction) play the role of an external magnetic field, which is no longer needed [10]. So this is a system which presents time reversal symmetry, and we can expect that only materials with a great spin-orbit coupling shall be topological insulators.

TI's can lead to a great technological advance, due to the intriguing properties this class of materials presents. Among the possibilities of applications using TI's, stand out the quantum computation and "spintronics", where not only the electric current carries information, but also the spins of electrons [6].

2.1.1 General properties

The bulk of a topological insulator presents an energy gap at its band structure, so behaves just like an ordinary insulator. However, as a result of the spin-orbit interaction, there are metallic edge states, which are robust against adiabatic changes in the Hamiltonian, such as deformations in the sample or addition of non-metallic impurities.

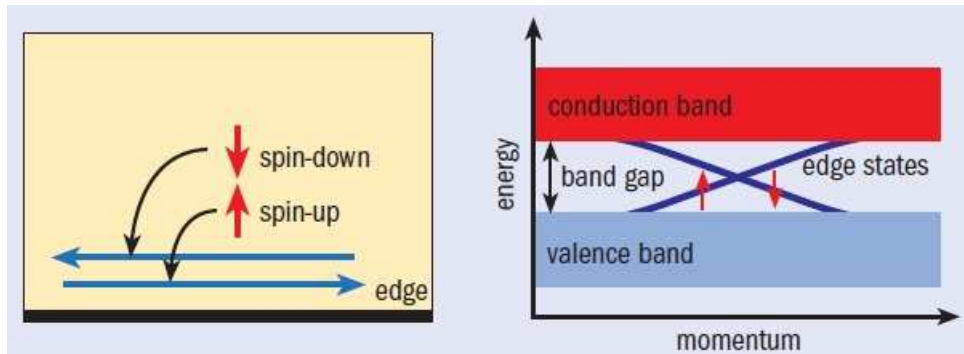


Figure 2.1: 2-D topological insulators have gapped structure band at the bulk, but edge metallic states which lies inside the bulk insulating gap. Electrons with anti-parallel spins propagate at opposite directions, due to the time reversal symmetry. (Source: Ref. [7])

We saw that the QH state has "chiral" edge states, in which electrons propagate in one direction only. Differently from what happens in the QH state, at 2-D topological insulators electrons with anti-parallel spins propagate in opposite directions at the edges of a sample (Fig. 2.1), leading to a zero Hall conductance because spin-up and spin-down electric currents cancel each other [1, 10]. These helical edge states come in Kramers doublets, and TR symmetry ensures the crossing of their energy levels at special points in the Brillouin zone. Due this level crossing, a topological insulator can

not be adiabatically deformed into that of a topologically trivial insulator [13].

Quantum Hall edge states do not allow backscattering due to the absence of a backward chiral state. A natural question is whether spin Hall quantum states allow backscattering, since now there are counter-propagating edge states. Although a QSH edge consists of both backward and forward movers, backscattering by nonmagnetic impurities is forbidden. To understand why this happens, let's begin with a simple analogy from optical physics. Lenses with antireflection coating have a thin film which allows the refracted light beams to be reflected too, so the two reflected beams interfere with each other destructively, leading to zero net reflection and thus perfect transmission (Fig. 2.2a). However, this effect is not robust, and depends on the thickness of the coating, which must be adjusted to match the optical wavelength.

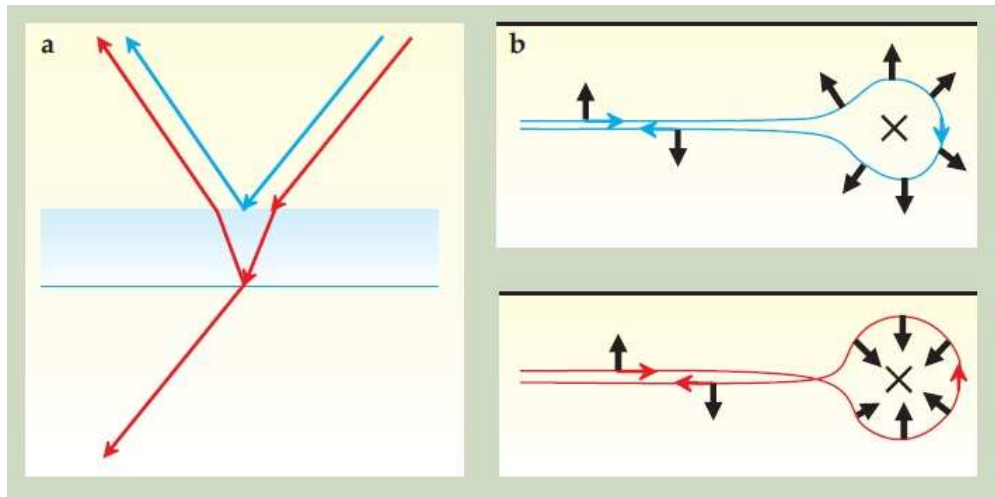


Figure 2.2: a) Destructive interference of light beams in antireflection lens. b) There are two possible paths for electrons to be backscattered by a nonmagnetic impurity, but these paths have a phase difference of -1 at their wavefunctions, which leads to a destructive interference of the two paths. Source: [8]

Just like reflection of photons by a surface, electrons can be reflected by an impurity, and different reflection paths interfere with each other. As shown in Fig. (2.2b), electrons in a QSH state can turn the impurity by two distinct paths, either clockwise or counter-clockwise, which leads to a rotation of π or $-\pi$ at its spin. In both cases the electron ends up at the backward state which inverted spin, but the two paths differ by a full $\pi - (-\pi) = 2\pi$ rotation of the electron spin. It is known that a full 2π rotation of a fermion spin change the sign of the wavefunction, so the two backscattering paths always interfere destructively, leading to a perfect transmission. This prohibition

of backscattering is robust, and we say that the helical edge states are topologically protected by time reversion symmetry. Of course, if we have a magnetic impurity, the time reversal symmetry is broken and the argument above no longer applies [8].

2.1.2 Fractional charge and quantized current

The beautiful phenomena of elementary excitation with half of the electronic charge can also be seen in a 2-D topological insulator. A consequence of the Su-Schrieffer-Heeger (SSH) model is that, for spinless fermions, a charge domain wall induces an elementary excitation with one-half charge [14]. Conventional materials, however, have two possible spin states. This doubling at the degrees of freedom (Fig. 2.3a) makes that the domain wall only carries integer charge. Helical edge states in topological insulators, on the other hand, have only two degrees of freedom, since momentum and spin are locked (Fig. 2.3b). Therefore, topological insulators can have elementary excitations with one-half charge [15].

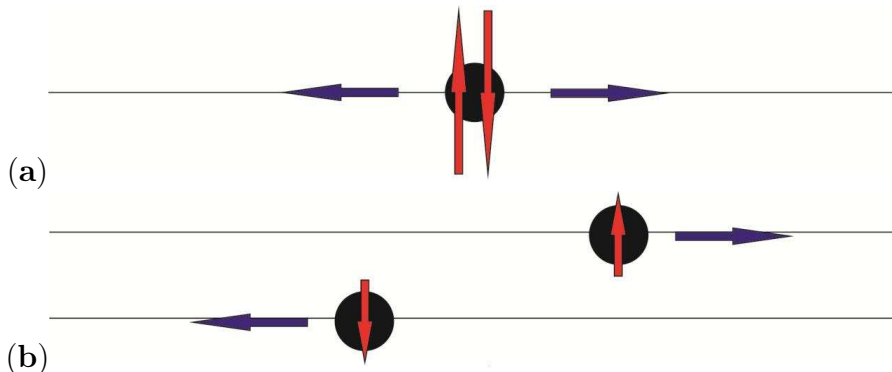


Figure 2.3: a) In conventional materials, 2 movement directions and 2 spin orientations (4 degrees of freedom) are present for each electron. b) Helical edge states present only two degrees of freedom due to the spin-momentum locking.

In the absence of TR symmetry, a magnetic field generates the following mass terms at the Hamiltonian:

$$H_M = \int dx \psi^\dagger \sum_{a=1,2,3} m_a(x,t) \sigma_a \psi = \int dx \psi^\dagger \sum_{a,i} t_{ai} B_i(x,t) \sigma_a \psi,$$

where the coefficient matrix t_{ai} is determined by the coupling of the edge states to the magnetic field. According to the work of Goldstone and Wilczek [16], at zero temperature the ground-state charge density and current in a background field $m_a(x,t)$

is given by

$$j_\mu = \frac{1}{2\pi} \frac{1}{\sqrt{m_\alpha m^\alpha}} \epsilon^{\mu\nu} \epsilon^{\alpha\beta} m_\alpha \partial_\nu m_\beta, \quad \alpha, \beta = 1, 2.$$

With $\mu, \nu = 0, 1$ corresponding to the time and space components, respectively. Parametrizing $m_1 = m \cos \theta$ and $m_2 = m \sin \theta$, the response equation is simplified to:

$$\rho = \frac{1}{2\pi} \partial_x \theta(x, t), \quad j = -\frac{1}{2\pi} \partial_t \theta(x, t).$$

Such a response is “topological” in the sense that the net charge Q in a region $[x_1, x_2]$ at time t depends only on the boundary values of $\theta(x, t)$ i.e. $Q = [\theta(x_2, t) - \theta(x_1, t)]/2\pi$. In particular, a half-charge $\pm e/2$ is carried by an anti-phase domain wall of θ , as shown in Fig. (2.4A). Similarly, the charge pumped by a purely time-dependent $\theta(t)$ field in a time interval $[t_1, t_2]$ is $\Delta Q_{\text{pump}}|_{t_1}^{t_2} = [\theta(t_2) - \theta(t_1)]/2\pi$. When θ is rotated from 0 to 2π adiabatically, a quantized charge e is pumped through the 1-D system, as shown in Fig. (2.4B).

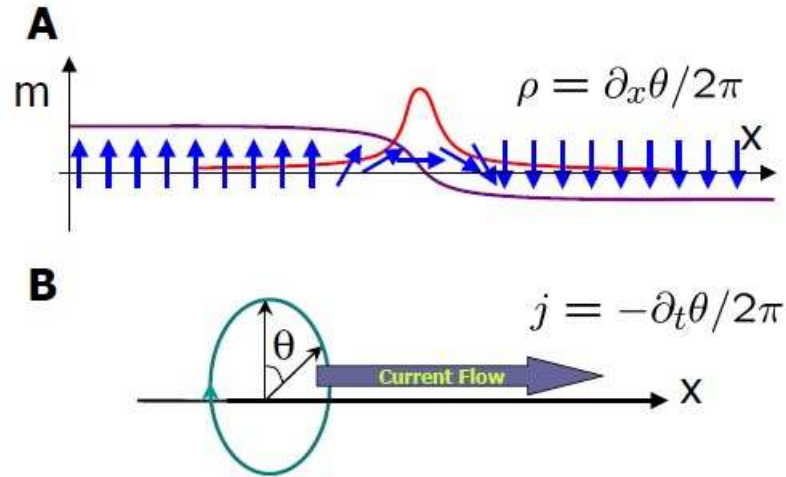


Figure 2.4: A) If the domain wall is anti-phase, it carries half of the electronic charge. The blue arrows show the magnetic domain wall configuration and the red curve shows the charge density distribution. B) A rotation in the magnetic field where θ goes from 0 to 2π induces the pump of a quantized charge e through the 1-D system. The blue circle with arrow shows the magnetic field rotation trajectory. (Source: [15])

2.1.3 Spin-charge separation

Another interesting effect which can occur in a 2-D topological insulator is that of the separation between spin and charge. This means a spacial separation, and this kind of excitation is one of the great appeals of condensed matter physics.

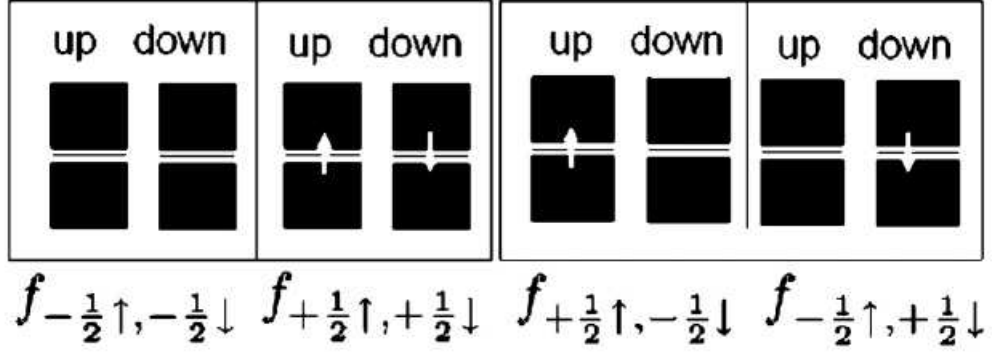


Figure 2.5: There are four different types of fluxons. The notation, e.g., $f_{+(1/2)\uparrow, -(1/2)\downarrow}$, means that the spin-up zero mode is filled while spin-down zero mode is empty. (Source: Ref. [17]).

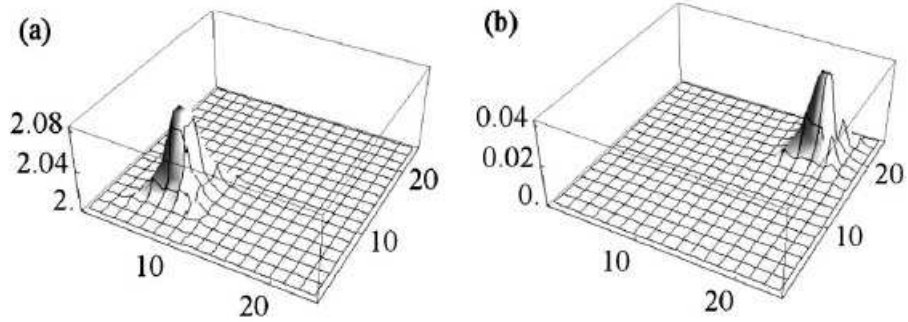


Figure 2.6: The a) charge and b) spin densities of a pair of fluxons on a 24×24 lattice with periodic boundary condition. The fluxon at coordinate $(6, 6)$ is $f_{+(1/2)\uparrow, +(1/2)\downarrow}$, it has charge 1 and $S_z = 0$. The fluxon at $(18, 18)$ is $f_{+(1/2)\uparrow, -(1/2)\downarrow}$, it has charge 0 and $S_z = 1/2$. The figure illustrates the spin-charge separation in real space. (Source: Ref. [17])

Considering the adiabatic insertion of a π gauge flux in the QSH state, two independent research groups [17, 18] demonstrated (in 2008) the existence of spin-charge separated quasi-particle excitations which are exponentially localized near the flux. These solitons are shown to have Bose statistics and are called “fluxons”. When fluxons are mobile their quantum statistics becomes important, and are determined by their statistics through explicit computation of the Berry phase. There are four different types of fluxons (Fig. 2.5) with the following quantum numbers: charge 1, $S_z = 0$; charge -1 , $S_z = 0$ (these two are called chargeons); charge 0, $S_z = 1/2$; charge 0, $S_z = -1/2$ (these are called spinons). Fig. (2.6) shows the charge and spin density profiles for a pair of fluxons.

2.2 Three-dimensional topological insulators

The unusual and exciting properties of topological insulators encouraged a lot of fruitful researches about these materials. An impressive fact is that those properties are not restricted to the bi-dimensional plane, and topological order also occurs in three-dimensional materials with a strong spin-orbit couple. Indeed, in 2006 there were three independent theoretical groups [19, 20, 21] which discovered that the topological characterization of the quantum spin Hall state has a natural generalization in three dimensions. In 2007, this phase was predicted in several real materials [22], and in 2008 it was reported [23] the experimental discovery of the first 3-D topological insulator in $\text{Bi}_{1-x}\text{Sb}_x$ [6]. A few examples of 3-D topological insulators are bismuth selenide (Bi_2Se_3), bismuth telluride (Bi_2Te_3) and antimony telluride (Sb_2Te_3).

2.2.1 General properties

Similar to the bi-dimensional ones, 3-D TI's bulk states are fully gapped, but there are topologically protected surface states. The surface electronic structure of a topological insulator is similar to graphene, except rather than having four Dirac points, there is just a single Dirac point. These surface states support electronic motion in any direction along the surface, but the direction of the electrons' motion uniquely determines its spin direction and vice versa, so they are “helical” in the sense that their spin is always perpendicular to their momentum and both are tangent to the surface (Fig. 2.7) [6, 7, 13].

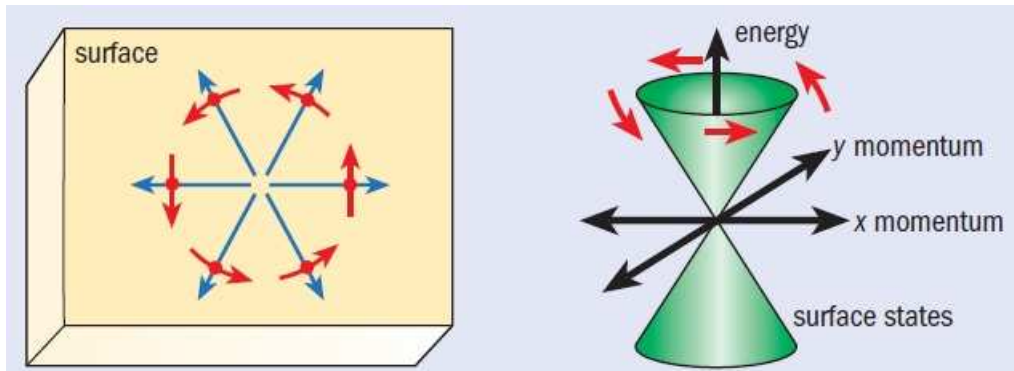


Figure 2.7: Electrons in a 3-D topological insulator are allowed to move in any direction along the surface, but its spin orientation (red) is related to its direction of motion (blue), in such a way that they are always perpendicular to each other and both tangent to the surface. (Source: Ref. [7]).

Also, 3-D topological insulators are robust and do not allow backscattering by a nonmagnetic impurity. This happens because Kramers pairs at \mathbf{k} and $-\mathbf{k}$ are forbidden to suffer backscattering, due to the time reversal symmetry [6].

The properties of topological insulators become much more interesting when we consider the possibility of inducing an energy gap at their surface states. This can be done by different ways, some of them are applying an external magnetic field in order to break the time reversal symmetry, or breaking the gauge symmetry due to proximity to a superconductor [6]. They will be briefly discussed here, but the topological magneto electric effect (TMEE) is so full of beautiful manifestations and important to this work that it will be dedicated a whole chapter to discuss it.

2.2.2 Surface quantum Hall effect

Applying a magnetic field normal to the surface would break the time reversal symmetry of the topological insulator surface state, inducing Landau levels at the electronic spectrum and leading to the quantum Hall effect. In this case, however, the Hall conductivity is equal and opposite when the Landau Level is full or empty, which is interpreted as a particle-hole symmetry. Landau levels for Dirac electrons have the guarantee to exist even at zero energy, and since the Hall conductivity increases by e^2/h when the Fermi energy crosses a Landau level, the Hall conductivity is *half-integer* quantized [6]:

$$\sigma_{xy} = (n + 1/2)e^2/h. \quad (2.1)$$

A similar effect happens with graphene, but there is an important difference. Graphene has 4 Dirac points, so the Hall conductivity is four times greater than equation (2.1), which leads to a net integer Hall conductivity. Otherwise, the surface of a 3-D topological insulator cannot have a boundary, since the top and bottom surfaces are always connected to each other, as shown in Fig. (2.8b). So the top and bottom surfaces share a chiral edge state, which carries the integer quantized Hall current.

Still, a half integer quantized Hall conductivity can be realized by the coating of the surface with a thin magnetic insulator film, which give rise to a local exchange field that lifts the Kramers degeneracy at the surface Dirac points. This opens a gap in the energy spectrum (Fig. 2.8c), and if the E_F is inside the gap, there is a Hall conductivity of $\sigma_{xy} = e^2/2h$. This is called the anomalous quantum Hall effect. At

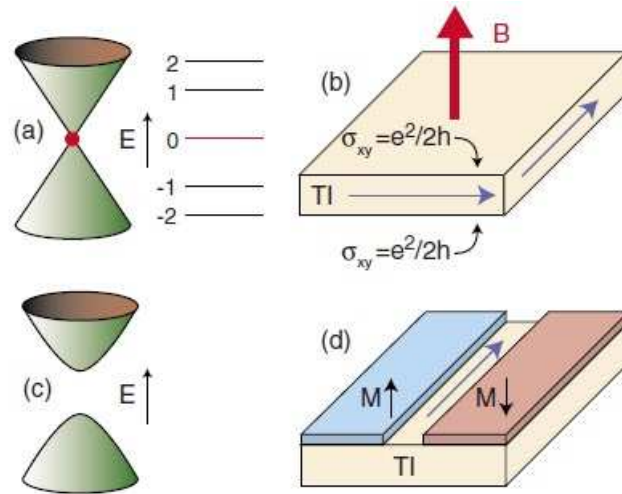


Figure 2.8: Quantum Hall effect on the surface of a topological insulator. a) An external magnetic field breaks the time reversal symmetry and gives rise to Landau levels. b) Top and bottom surfaces share a single chiral edge state, which has net integer quantized Hall conductivity. c) A thin magnetic insulator film induces an energy gap at the surface spectrum. d) A domain wall in the surface magnetization exhibits a chiral fermion mode. (Source: Ref. [6]).

an interface where the magnetization change its orientation, there can be a 1-D chiral edge state (Fig. 2.8d)[6].

2.2.3 Majorana fermions on topological insulators

As Majorana fermions have properties that can be very useful to quantum computing, it is important to mention that Majorana modes can take place at the interface between a topological insulator and a superconductor. In such configuration, Cooper pairs may tunnel from the superconductor to the surface, leading to an induced superconducting energy gap at the surface states. The resulting 2-D superconducting state is different from an ordinary superconductor because the surface states are not spin degenerate and contain only half the degrees of freedom of a normal metal. The surface superconductor does not violate time reversal symmetry, and its Cooper pairs have even parity [6].

Chapter 3

Topological magneto-electric effect (TMEE)

By coating the surface of a 3-D topological insulator with a thin magnetic film, where the magnetization is perpendicular to the surface, one induces an energy gap at the energy spectrum of the surface states, which leads to the quantum Hall effect. In reference [24], the authors have shown that such break in time reversal symmetry leads to the most striking phenomena of 3-D topological insulators, the so called topological magneto-electric effect (TMEE). Here, the electromagnetic response of the topological insulator is unusual, in the sense that an external electric (magnetic) field induces both polarization and magnetization at the sample, contrary to what happens with topologically trivial insulators.

3.1 A different way of inducing electric polarization and magnetization

A linear electromagnetic response of a conventional insulator which dielectric constant ϵ and magnetic permeability μ can be described by the effective action $S_0 = \frac{1}{8\pi} \int d^3x dt (\epsilon \mathbf{E}^2 + \frac{1}{\mu} \mathbf{B}^2)$. Where $\mathbf{E}(\mathbf{x})$ and $\mathbf{B}(\mathbf{x})$ are the electrical and magnetic field, respectively; and $d^3x dt$ is the volume element of space and time. As a result, the material responds to an external electric field with a polarization \mathbf{P} , and to a magnetic field with a magnetization \mathbf{M} . However, there is another term allowed in the effective action, which is quadratic in the electromagnetic field, contains the same number of derivatives of the electromagnetic potential, and is rotationally invariant; this term is

given by:

$$S_\theta = \left(\frac{\theta}{2\pi}\right) \left(\frac{\alpha}{2\pi}\right) \int d^3x dt \mathbf{E} \cdot \mathbf{B}. \quad (3.1)$$

Where α is the fine-structure constant, and θ is a phenomenological parameter in the sense of the effective Landau-Ginzburg theory. This term describes the magneto-electric effect, which is explained in reference [25]. In such effect, an electric field can induce a magnetization, and a magnetic field can induce an electric polarization.

Expressing $\mathbf{E}(\mathbf{x})$ and $\mathbf{B}(\mathbf{x})$ in terms of the electromagnetic vector potential, S_θ can be written as:

$$S_\theta = \frac{\theta}{2\pi} \frac{\alpha}{4\pi} \int d^3x dt \partial^\mu (\varepsilon_{\mu\nu\rho\tau} A^\nu \partial^\rho A^\tau). \quad (3.2)$$

Imposing periodic boundary conditions and time reversal symmetry, it can be shown that all time-reversal invariant insulators fall into two general classes, described by either $\theta = 0$ or $\theta = \pi$. These two classes are disconnected, and they can only be connected continuously by time-reversal breaking perturbations [24, 26].

When the surface of a 3-D topological insulator is coated with a thin ferromagnetic film, time-reversal symmetry is broken, and an energy gap opens up at the surface. In this case, the low-energy theory is completely determined by the surface term in Eq. (3.2). This surface term describes the quantum Hall effect on the surface. The Chern-Simons-Landau-Ginzburg theory of the quantum Hall effect establishes that the coefficient $\theta = 0$ leads to no Hall conductance at all, but $\theta = \pi$ gives a quantized Hall conductance of [27]:

$$\sigma_{xy} = \frac{e^2}{2h}. \quad (3.3)$$

A key difference between the surface half QH effect and the usual integer QH effect is that the former cannot be measured by a dc transport experiment, because the surface of a finite sample of 3-D topological insulator is always a closed manifold without an edge [13]. A physical manifestation of the magneto-electric effect is a drastic change in how the material reacts to an external electromagnetic field. An applied electric field induces a quantized Hall current on the surface, which in turn generates a magnetization in the sample. Also, an applied magnetic field generates an electric polarization. This unusual electromagnetic response of topological insulators constitutes the surprising topological magneto-electric effect (TMEE), which has some interesting physical manifestations that will be discussed in the next sections.

TMEE may be encompassed in the usual electrodynamics keeping the Maxwell

equations unaltered in form, with changes in the constitutive relations [26]:

$$\begin{aligned}\mathbf{D} &= \mathbf{E} + 4\pi\mathbf{P} - \{2\alpha P_3\mathbf{B}\} \\ \mathbf{H} &= \mathbf{B} - 4\pi\mathbf{M} + \{2\alpha P_3\mathbf{E}\},\end{aligned}\tag{3.4}$$

where α is the fine structure constant and P_3 is the electro-magnetic polarization [24]. In conventional insulators $P_3 = 0$, while in TIs $P_3 = \pm 1/2$. The direction of the surface magnetization determines the sign of P_3 (+ if pointing out the surface or - inward).

The simplest and intuitive example to see the manifestation of TMEE is that of a cylindrical topological insulator [24]. In order to break the TR symmetry, the curved surface must be coated with a thin ferromagnetic film, holding its magnetization perpendicular to the surface. The application of an external electric field \mathbf{E} along the symmetry axis gives rise to a quantized Hall current \mathbf{j}_{Hall} surrounding the topological insulator (Fig. 3.1a) that, according to Eq. (3.3), is given by:

$$\mathbf{j}_{Hall} = \frac{e^2}{2h}\hat{\mathbf{n}} \times \mathbf{E}.\tag{3.5}$$

Where $\hat{\mathbf{n}}$ is the unitary vector normal to the surface. This current is identical to the surface bound current generated by a constant topological magnetization response \mathbf{M}_t proportional to the electric field \mathbf{E} :

$$\mathbf{M}_t = -\frac{e^2}{2hc}\mathbf{E}.$$

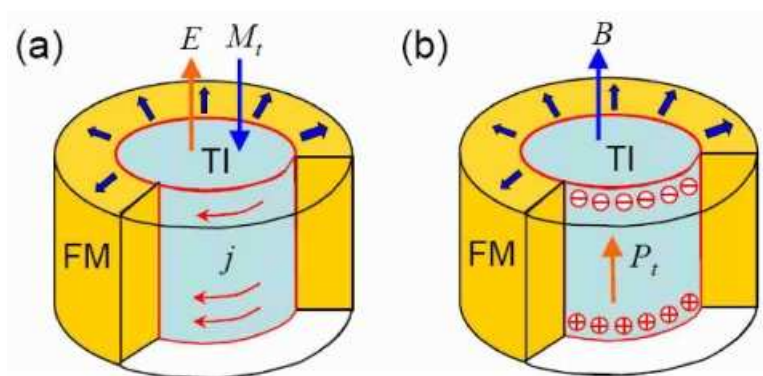


Figure 3.1: The TMEE manifests with electromagnetic topological responses that are independent on details of the system. a) Application of an external electric field induces a topological magnetization response. b) Application of an external magnetic field induces a topological electric polarization response. Source: (Ref. [13])

Similarly, the application of a magnetic field \mathbf{M} along the symmetry axis (Fig. 3.1b) leads to a topological electric polarization response \mathbf{P}_t :

$$\mathbf{P}_t = \frac{e^2}{2hc} \mathbf{B}.$$

The conventional Maxwell's equations, supplemented by constituent relations (3.4), give the complete description of the electrodynamics of the 3-D topological insulators [24].

The Hall current (Eq. 3.5) depends on the surface geometry, and its associated magnetic field may have special features. For instance, in a conical TI this current yields electric polarization that depends on the cone aperture angle, namely, under the same external conditions, wider ($\delta > 30^\circ$) and narrower ($\delta < 30^\circ$) cones appear to polarize in opposite directions [28].

3.2 Deflection of light by the surface of a topological insulator

TMEE plays an interesting role in interactions of light with the surface of topological insulators. Both transmitted and reflected polarized light are affected by the unusual form of the constitutive relations (3.4), having their plane of polarization rotated.

3.2.1 Faraday effect

It is known that the propagation of linearly polarized light through a medium with broken TR symmetry causes a rotation at the plane of polarization of the transmitted light. This is called the *Faraday effect* or *Faraday rotation* [25]. In topological insulators surfaces coated with a ferromagnetic film, TR symmetry is broken and such effect can be observed due to the TMEE.

Classically, light is basically propagating electromagnetic fields, and therefore must provoke an electromagnetic response when interacting with the surface of topological insulators, which is governed by the constituent relations from Eq. (3.4). The electric field of polarized light generates a magnetic field in the same direction, and the magnetic field creates an electric field in its direction. As the incident electric and magnetic fields are mutually perpendicular, the generated fields constitute orthogonal components of a resultant electromagnetic field, and the final effect is a rotation of θ_F at the plane

of polarization of the transmitted light (Fig. 3.2). The bulk of a topological insulator is invariant under TR symmetry, so once rotated at the surface, the light propagates through the material without any other rotation until it reaches the opposite surface or is fully absorbed by the medium [13].

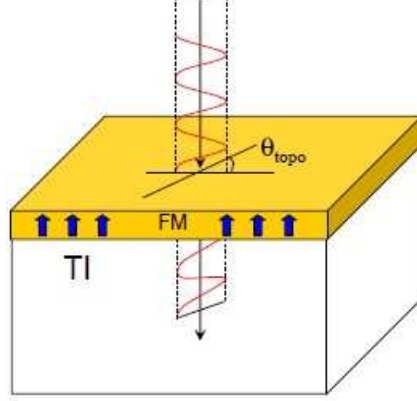


Figure 3.2: Illustration of the Faraday effect on the surface of a topological insulator, the transmitted light suffers a rotation of θ_F at its plane of polarization. (Source: Ref. [13])

The Faraday rotation angle θ_F can be calculated by solving Maxwell's equations with the modified constituent relations (Eq. 3.4). In the simplest case of a single interface between a trivial insulator and a semi-infinite topological insulator (Fig. 3.2), the rotation angle for light incident from the trivial insulator is given by [24, 29, 30, 31]:

$$\tan \theta_F = \frac{2\alpha P_3}{\sqrt{\epsilon_1/\mu_1} + \sqrt{\epsilon_2/\mu_2}},$$

where ϵ_1, μ_1 are the dielectric constant and magnetic permeability of the trivial insulator, and ϵ_2, μ_2 are those of the topological insulator.

3.2.2 Kerr effect

Similar to the Faraday effect, there can be a rotation of θ_K at the plane of polarization of light reflected by a surface, which is known as the magneto-optical *Kerr effect*, or *Kerr rotation* [25]. Kerr effect also takes place on the surface of a topological insulator, since TR symmetry has been broken by coating the surface with a ferromagnetic film. The physical explanation relies on the same arguments of the Faraday effect, and calculation of the Kerr angle θ_K by solving Maxwell's equations with the constitutive relations (Eq. 3.4) leads to [24, 29, 30, 31]:

$$\tan \theta_K = \frac{4\alpha P_3 \sqrt{\epsilon_1/\mu_1}}{\epsilon_2/\mu_2 - \epsilon_1/\mu_1 + 4\alpha^2 P_3^2},$$

where the constants and the direction of the incident beam are the same defined before for the expression of θ_F .

Such topological electromagnetic responses compete with the usual nontopological electromagnetic effects, and in general they are much smaller in magnitude, which makes them too hard to be observed in experimental laboratories. Indeed, despite the TMEE being proposed in 2008, it was only confirmed experimentally in the end of the last year (October 2015 [32], and also in march 2016 by two independent groups [33, 34]), through the observation of the Faraday and Kerr effect.

3.3 Magnetic monopoles (and dyons)

The electromagnetic theory is known to be one of the most symmetric theories of humankind, or almost there. A simple look at the Maxwell's equations is enough for us to see that electromagnetism is not symmetric only because of the absence of magnetic charge. Magnetic monopoles have been discussed for several years, wherein Pierre Curie pointed out in 1894 that they could exist, despite not having been seen so far [35]. The nonexistence of these particles has intrigued the notable physicist Paul A.M. Dirac, who have shown that existence of magnetic monopoles would explain why electric charges appears only as integer multiple of the electronic charge [36]. Today, magnetic monopoles are predicted to exist in superstring theories [37], but remains not detected experimentally. Some condensed matter systems contain quasi-particles that behave like magnetic monopoles, as in some spin ice models [38, 39, 40], which is the closer we could get, but they are not real magnetic monopoles, so we have no proof that they really exist.

Another surprising consequence of the TMEE concerns to the induction of image magnetic monopoles inside the bulk of a topological insulator. Consider for instance a point-like electric charge q in the bulk of a conventional insulator, in such a way that the charge is located a distance d above the semi-infinite plane interface between the conventional insulator and a topological insulator surface with broken TR symmetry (Fig. 3.3). The lower-half space ($z < 0$) is occupied by the topological insulator with a dielectric constant ϵ_2 and a magnetic permeability μ_2 , whereas the upper-half space ($z > 0$) is occupied by the conventional insulator with a dielectric constant ϵ_1 and a magnetic permeability μ_1 .

To find the electric and magnetic fields of this configuration, the method of images

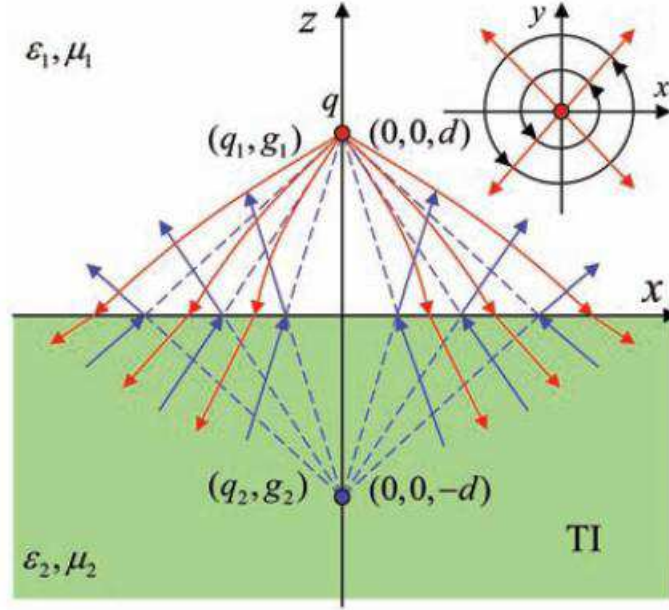


Figure 3.3: Electric charge near the plane interface between a topologically trivial insulator and a three-dimensional topological insulator. The electric field of the point-like charge induces the usual polarization at the topological insulator plus a surface quantized Hall current. This current generates a magnetic field that can be described by image magnetic monopoles. The red lines represent the electric field, the blue lines represent the magnetic field and the circulating black lines represent the surface Hall current. (Source: Ref. [26]).

[41] can be applied, since Maxwell's equations and the standard boundary conditions constitute a complete boundary value problem, as long as we are considering the constitutive relations given by Eq. (3.4). Assuming that in the lower-half space, the electric field is given by an effective point charge q/ϵ_1 and an image charge q_1 at $(0, 0, d)$, whereas the magnetic field is given by an image magnetic monopole g_1 at $(0, 0, d)$. In the upper-half space, the electric field is given by q/ϵ_1 at $(0, 0, d)$ and an image charge q_2 at $(0, 0, -d)$; the magnetic field is given by an image magnetic monopole g_2 at $(0, 0, -d)$.

In order to satisfy the Maxwell's equations and the boundary conditions, the image electric charges and magnetic monopoles must satisfy [26]:

$$q_1 = q_2 = \frac{1}{\epsilon_1} \frac{(\epsilon_1 - \epsilon_2)(1/\mu_1 + 1/\mu_2) - 4\alpha^2 P_3^2}{(\epsilon_1 + \epsilon_2)(1/\mu_1 + 1/\mu_2) + 4\alpha^2 P_3^2} q,$$

$$g_1 = -g_2 = -\frac{4\alpha P_3}{(\epsilon_1 + \epsilon_2)(1/\mu_1 + 1/\mu_2) + 4\alpha^2 P_3^2} q.$$

These solutions show that for an electric charge near the surface of a topological insulator, both an image magnetic monopole and an image electric charge will be

induced, whereas in conventional insulators only an electric image charge appears. Note that the magnitudes of the image magnetic monopole and image electric charge satisfy the relation $q_{1,2} = \pm(\alpha P_3)g_{1,2}$. This kind of relation is also satisfied by particles known as dyons [42], which have both electric and magnetic charge. So it is reasonable to say that an electric charge near the surface of a topological insulator with broken TR symmetry induces an image dyon inside its bulk. The reader could question about the dyon located at $(0, 0, d)$, which is indeed induced, but as this is an analysis by the method of images it just make sense to talk about this dyon when the observer is inside the topological insulator, which is not usually the case.

The image magnetic monopole in a TI is not an elementary excitation of the system, neither an emergent from the collective behaviour, it is an artificial particle that describes the physical effects associated with the TMEE. In this sense, it is different from the magnetic monopoles in spin ice where it is an elementary excitation that emerges from the collective behaviour of the microscopic degrees of freedom [38, 39, 40], or of the monopole proposed in a nanoscopically thin magnetic needle where is created an approximation of a magnetic monopole in free space [43].

The method of images is a very powerful technique to find the final state of the system, but it lacks details about the physical origin of these image magnetic monopoles. To understand what really happens we must resort to the TMEE, in which an external electric field \mathbf{E} generates a topologically quantized Hall current on the surface of the topological insulator. In these configuration with a plane interface, the Hall current \mathbf{J}_{Hall} is circulating (Fig. 3.3) and given by Eq. (3.5)[26]:

$$\mathbf{j}_{Hall} = P_3 \left(\frac{e^2}{h} \right) \left(\frac{q}{1 + \alpha^2 P_3^2} \right) \frac{r}{(r^2 + d^2)^{\frac{3}{2}}} \hat{\mathbf{e}}_\varphi, \quad (3.6)$$

where it was taken $\epsilon_1 = \epsilon_2 = \mu_1 = \mu_2 = 1$, in order to simplify the mathematical expression and focuses only at the physic interpretation. The electric field of the real point-like electric charge penetrates the material, inducing not only the usual polarization \mathbf{P} , but also a magnetic field generated by the Hall current. The resulting electric and magnetic fields on each side of the surface are exactly the same of those generated by the image charges on the opposite side, so we can say that the problem is completely determined by the image charges configuration. In order to verify this equivalence we have calculated the magnetic field generated by the Hall current, along the z-axis. Using equation (3.6) in Biot-Savart's law [41], we are lead to:

$$\mathbf{B}(z) = \frac{2\pi e^2}{c h} \frac{q}{1 + \alpha^2 P_3^2} \frac{1}{(z + d)^2} \hat{\mathbf{z}}. \quad (3.7)$$

This result shows that the magnetic field varies with distance as $1/(z+d)^2$, so it is in fact the one generated by a magnetic monopole located in $z = -d$. This behavior may seem contradictory, since we are familiarized with the $1/z^3$ leading term for fields generated by closed electric currents. However, the monopole term in multipole expansions only vanishes if the current is enclosed, which is not the case. Here, the Hall current exists for any value of r along the surface, extending from $r = 0$ to $r = +\infty$.

All these results were obtained starting from Maxwell's equations, including $\nabla \cdot \mathbf{B}$, so it must be satisfied everywhere in the space. In other words, the magnetic field integrated over a closed surface must vanish. Indeed, it can be seen that this is the case by considering the closed surface of a sphere with radius a that encloses a topological insulator. Inside the closed surface, there is not only a image magnetic monopole charge, but also a line of magnetic charge density whose integral exactly cancels the point image magnetic monopole. However, when the separation between the electric charge and the surface (d) is much smaller than the spherical radius (a), the magnetic field is completely dominated by the image magnetic monopole, and the contribution due to the line of magnetic charge density is vanishingly small [26].

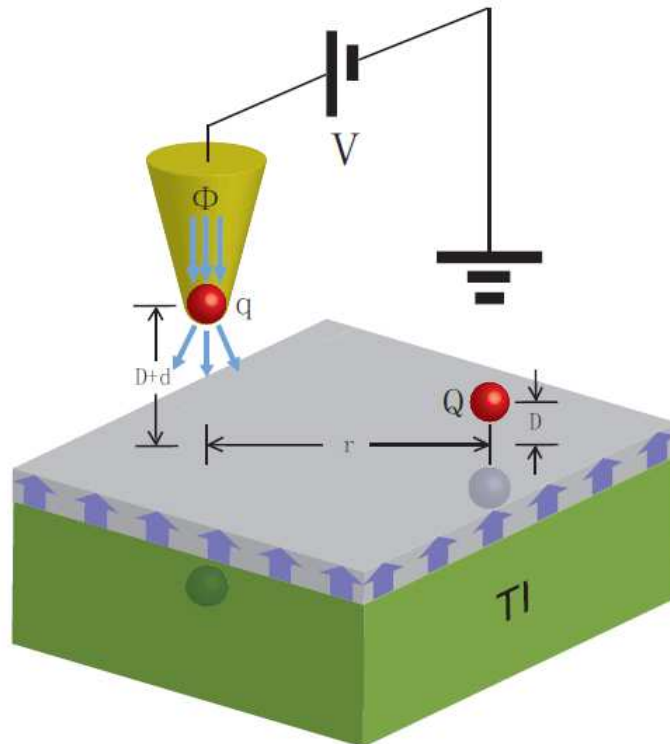


Figure 3.4: Illustration of an experimental apparatus that can be used to measure the magnetic field distribution generated by an image magnetic monopole, next to the surface of a topological insulator. (Source: Ref. [26])

The image magnetic monopole can be observed experimentally using a magnetic force microscope (MFM). Consider a localized electrically charged impurity Q placed a small distance D above the surface of a topological insulator, coated with a thin ferromagnetic film (Fig. 3.4). The tip of the MFM is able to measure the magnetic field distribution of the image monopole. However, the charge of the impurity also generates an electric force to the tip. The contribution of the the image monopole can be distinguished from other trivial forces by scanning both the tip position r and voltage V . When the position $r \gg D$, the image monopole magnetic field leads to more dominant contribution and can be observed by the tip [26].

Chapter 4

Semi-spherical topological insulator

In this work, we have investigated the electromagnetic configuration generated by a point-like electric charge q' near the concave interface between a conventional insulator and a semi-spherical topological insulator, because it has a special point in which can occurs an interesting effect. Naturally, it is the focus of the semi-sphere. Due to this particular geometry and the cross product on Eq. (3.5), it is expected a change in the monopole's sign when the electric charge crosses this point. This effect is typical from negative curved surfaces, since at those with positive curvature the Hall current shall circulate always in the same direction, no matter the distance from the electric charge.

4.1 TMEE on the semi-spherical TI surface

Let the z-axis be placed over the symmetry axis, with positive side pointing in the opposite direction to the surface, and the origin of the coordinate system in the focus of the semi-sphere. To simplify, place the electric charge over the z-axis, at position z_0 (Fig. 4.1).

We shall use only the first order contribution to the electric field, which is given by the Coulomb electric field with an effective charge $q = q'/\epsilon_1$, that is $\mathbf{E} = q \frac{\vec{r} - z_0 \hat{z}}{|\vec{r} - z_0 \hat{z}|^3}$. Here, ϵ_1 is the dielectric constant of the conventional insulator, \vec{r} represents an arbitrary point, and z_0 gives the electric charge location. Using this in Eq. 3.5, one can easily find:

$$\mathbf{J}_{Hall} = -\frac{e^2}{2h} (qz_0) \frac{\sin \theta}{(R^2 + z_0^2 - 2Rz_0 \cos \theta)^{3/2}} \hat{e}_\varphi, \quad (4.1)$$

where θ and φ are the spherical *polar* and *azimuthal* angles, respectively. R is the semi-sphere radius, and the topological insulator surface extends from $\theta = \frac{\pi}{2}$ to $\theta = \pi$

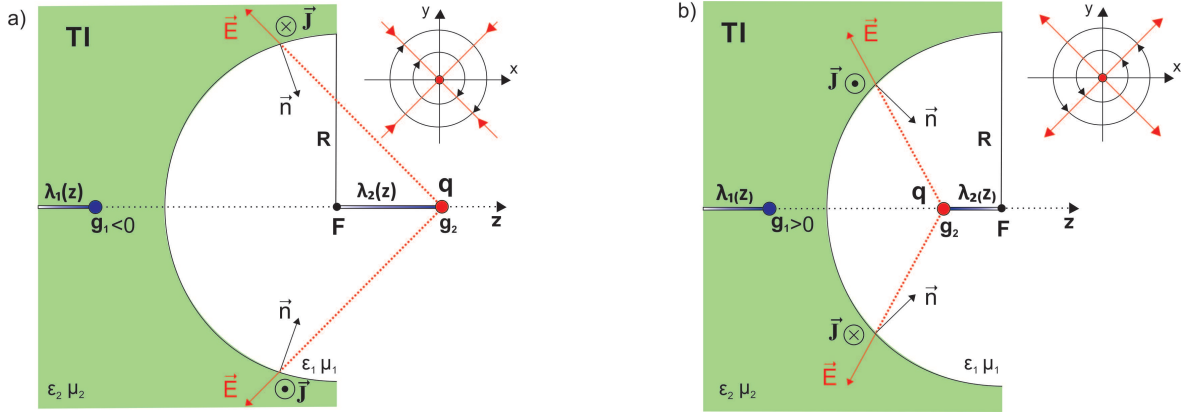


Figure 4.1: Illustration of magnetic monopoles charge reversion as the point-like electric charge crosses the semi-sphere focus. In figure a), $z_0 > 0$, so the Hall current is always clockwise (see inset), which indicates a negative image magnetic monopole. In figure b), $z_0 < 0$, so the Hall current is counter-clockwise, and the monopole has positive magnetic charge (see inset). Notice that in figure a), the tangential components of the electric field point radially inwards, what never happens in positively curved surfaces. The red lines represent the electric field and the black circles represent the circulating surface current \mathbf{J} . The magnetic field lines were omitted for simplicity. z_0 is the position of the electric charge q , relative to the origin of the coordinate system. μ_1 and ϵ_1 (μ_2 and ϵ_2) are the magnetic permeability and the dielectric constant of the conventional insulator (topological insulator), respectively.

with azimuthal symmetry.

Before any calculations, we can have a good qualitative understanding of what happens when the electric charge crosses the semi-sphere's focus F. Looking at geometry of the topological insulator, we can expect that there will be a magnetic monopole g_1 , plus a line of magnetic charge density $\lambda_1(z)$ extending from the monopole to negative infinity in the image charge configuration inside the bulk, as it happens for spherical TI's [26].

The Maxwell's equations, which includes $\nabla \cdot \mathbf{B} = 0$ (\mathbf{B} is the magnetic field), must be satisfied everywhere in the real space, so the magnetic flux over a surface involving the topological insulator must vanish. As a consequence, the total charge in the line must exactly cancels the charge of the magnetic monopole, with opposite sign, i.e. $\int \lambda_1(z) dz = -g_1$. So we can assure that the dominant contribution to the magnetic field is due to the monopole (which is closer to the region of interest), and the sign of the z component of the magnetic field also determines the monopole's sign. Therefore, the

clockwise or counter-clockwise direction of the Hall current indicates if the monopole is negative or positive, respectively.

As we can easily see from Eq. (4.1), the electric charge position (above or below $z=0$) completely determines the current sign, and therefore the sign of the magnetic monopole. When the charge is exactly in the focus, there is no current and therefore no images magnetic charges. But when it crosses this point, the sign of the magnetic monopole is reversed, and also the sign of $\lambda_1(z)$.

4.2 Magnetic field analysis and image magnetic charge configuration

An expression to the magnetic field along the z axis is obtained (Appendix) by using Eq. (4.1) in Biot-Savart's law. Its behaviour is shown in Fig. (4.2) for several values of z_0 , where we took $R = 1$, so the intersection of the axis with the surface occurs in $z = -1$. Notice that when the electric charge crosses the semi-sphere focus, the magnetic field changes its sign, evidencing the sign reversion of the magnetic monopole.

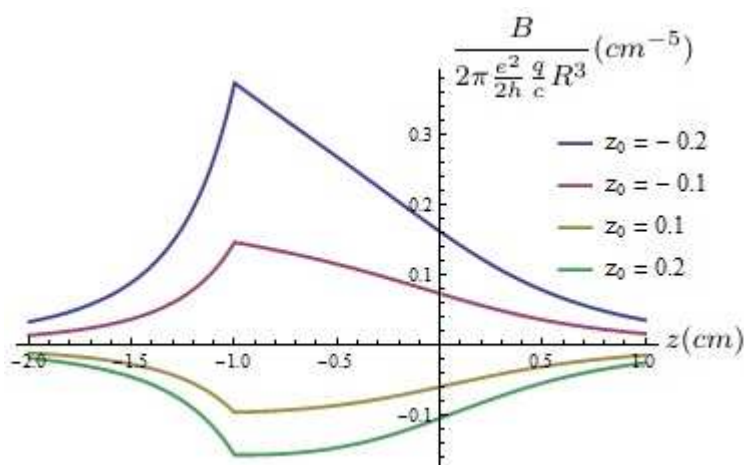


Figure 4.2: Behaviour of the magnetic field along the z -axis, generated by the Hall current on the semi-spheric interface. It is shown for different values of z_0 , evidencing the change in the field's sign when the electric charge crosses the semi-sphere focus ($z = 0$). Intersection of the z -axis with the surface occurs at $z = -1$, since $R = 1$. In the vertical axis label, c is the speed of light.

In Fig. (4.3), it can be seen that the closer the charge is from surface, more and more we have a magnetic field similar to the one of a point-like charge. This suggests

that in such case, the density magnetic charge of the line is widespread along its length so what we effectively see is the magnetic monopole alone.

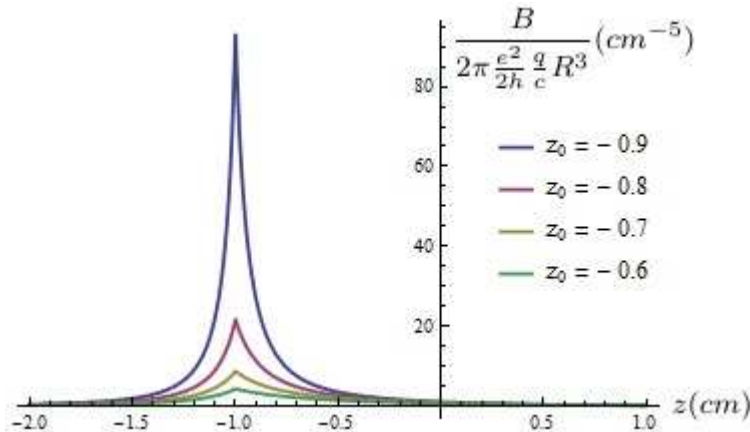


Figure 4.3: The electric charge is brought near the surface, and the magnetic field approaches to the one of an image point-like magnetic charge.

We have proposed an image magnetic charge configuration for this system, in the case in which $-R < z_0 < 0$. The magnetic field generated by a monopole g_1 located at $z = \frac{R^2}{z_0}$ (reverse point) and a line of magnetic charge $\lambda_1(z)$ along the z axis (both located inside the topological insulator), extending from the monopole to negative infinity, must completely describes the real one, but only in the region outside the topological insulator.

Considering g_1 as a parameter, in Fig. (4.4) we compare the magnetic field produced by the Hall current induced in the surface with the magnetic field produced by the magnetic monopole near the reverse point. If we consider the magnetic monopole in the reverse point, the agreement between the magnetic fields is very good, justifying the magnetic monopole image picture to describe the magnetic field. If we look at points far away from the surface, where $z \gg R$, it is easy to show that the magnetic field decreases as $1/z^3$, and not as the $1/z^2$ expected for a monopole. Indeed, Fig. (4.5) shows the mismatch between the fields in great distances. Here, unlike what happens in the plane surface, the Hall current is limited between $\theta = \frac{\pi}{2}$ and $\theta = \pi$, so the multipole expansion has no monopole contribution. In the image charges picture, this happens because seen from so far away the line of magnetic charge does not seem to be spread, but concentrated at just one point, so the field generated by the monopole and the line of magnetic charge density becomes that one of a magnetic dipole. This is quite comprehensible as it also happens next to the tip of a magnetic needle (which

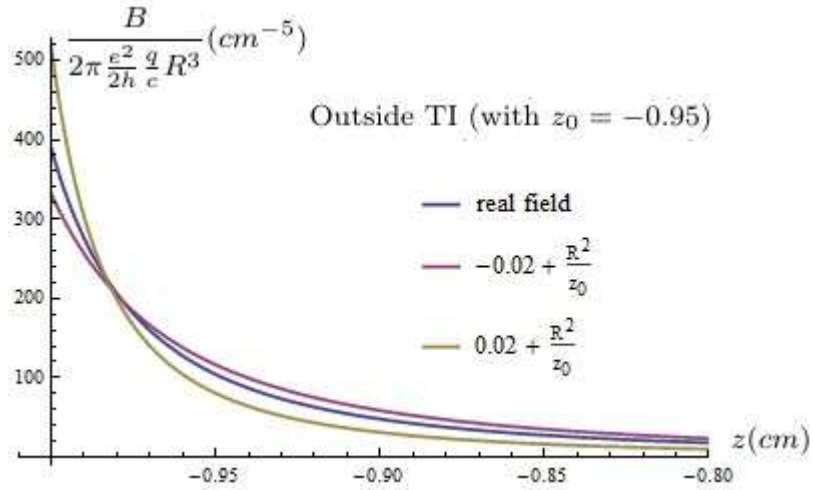


Figure 4.4: Comparison between the magnetic fields generated by the Hall current and by the image magnetic monopole g_1 near the reverse point. We consider the electric charge very close to the surface ($z_0 = -0.95$). The fields are shown in the same region as the electric charge, while the monopole is located inside the topological insulator. If the magnetic monopole is exactly in the reverse point, the concordance between the Hall current's magnetic field and the magnetic monopole's field is perfect.

is a kind of long dipole) [43].

The magnetic field inside the topological insulator is completely described by a monopole g_2 located at the same point as the electric charge ($z = z_0$), plus a line of magnetic charge $\lambda_2(z)$ along the z axis (both located outside the topological insulator), extending from the monopole to the focus F (Fig. 4.1). When the electric charge is close to the surface, the fields produced by the magnetic monopole and the Hall current fits very well, showing that the monopole contributes much more to the field than the line of magnetic charges, as in the case discussed before, where the magnetic monopole is inside the TI.

In the limit that the charge approaches the surface, the position of the image monopole g_1 becomes $\frac{R^2}{z_0} = \frac{R^2}{-R+\varepsilon} \approx -R - \varepsilon$, so we are led to the same planar case described in Ref. [26]. This is in concordance with the fact which states that when the distance between the electric charge and the topological insulator's surface is much smaller than its curvature radius, the magnetic field is completely determined by the magnetic monopole, since locally we have a plane surface.

The magnetic monopole induced by an electric charge near a convex surface (spherical) decreases with the inverse of the distance between the electric charge and the

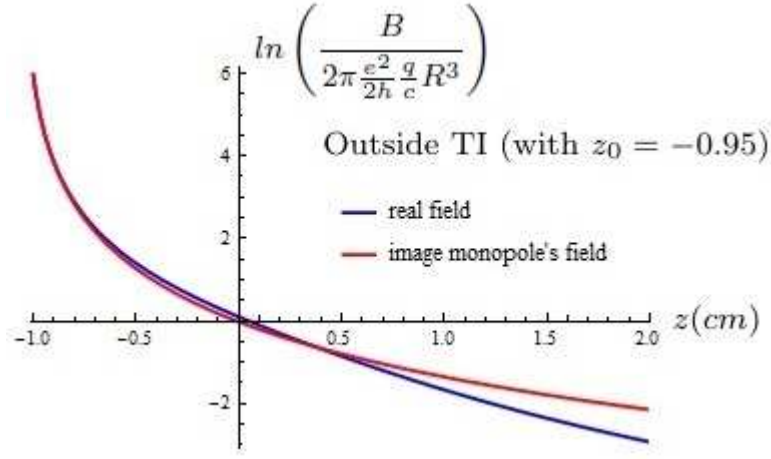


Figure 4.5: Comparison between $\ln B$ for both the fields generated by the Hall current and by the magnetic monopole. The electric charge is located close to the surface of the topological insulator ($z_0 = -0.95$). Note that when looking far away from the surface, the fields mismatch.

center of the spherical surface [26]. Here, due to negative curvature, the intensity of the magnetic monopole grows linearly with the distance between the electric charge and the surface of the TI, as long as the electric charge is very close to the surface (Fig. 4.6). However, there is no Hall current when the electric charge is located exactly in the focus, and therefore, no magnetic monopole at all ($g_1 = 0$), so we expect that this intensity reaches a maximum when z_0 is somewhere in the region between the surface and the focus.

Moving the electric charge away from surface, the monopoles magnetic fields shift from the real one because the lines of magnetic charges are concentrated next to the monopoles and cannot be neglected (Fig. 4.7). As these charges have opposite signs to the monopoles, the resultant effect is to decrease their fields.

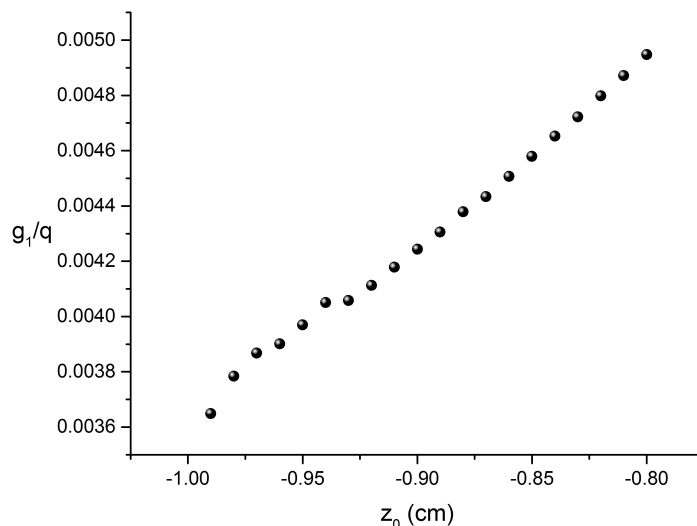


Figure 4.6: Variation of the magnetic monopole intensity with the distance between the electric charge and the TI surface. Notice that g_1 grows linearly with the distance in the region where the magnetic monopole picture is valid.

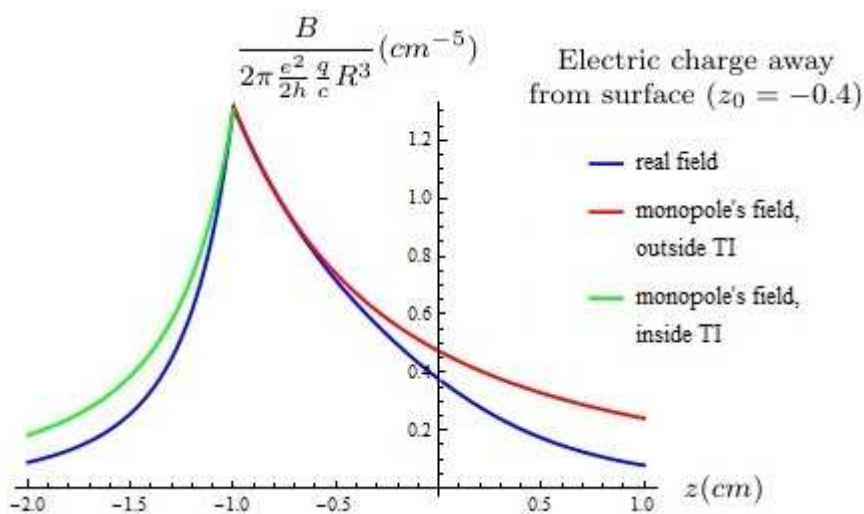


Figure 4.7: Comparison between the real magnetic field, generated by the Hall current on surface, and the fields of the image monopoles, when the electric charge is not close to the surface, but still inside the concavity ($z_0 = -0.4$). In this situation, the field generated by the lines of magnetic charge density are not negligible, so the curves in the graph do not fit very well, since we are taking in account only the field generated by the magnetic monopole.

4.3 Conclusions and Prospects

Due to the complicated geometry of the surface and the expression for the magnetic field, it is hard to determine an expression to the image line of magnetic charge or even the monopoles. However, we know their location by the very good fitting among their magnetic fields and the real one when the charge is close enough to the surface and the line of magnetic charges contribution becomes negligible.

We have presented valid arguments that when the charge is inside the cavity, the positions of the monopoles and lines of magnetic charges keep the same that in the case of spherical topological insulators, although their magnitudes are different. If the charge is too close to the surface, locally we have a plane interface, so the solution is the same than that for a plane interface. The fields generated by the lines of image magnetic charge density are not negligible when the electric charge is away from surface, so the fields generated by the monopoles shift from the real one. When looking far away from surface, the monopole and the line of charges together looks like a magnetic dipole and the field decreases as $1/z^3$.

When the electric charge approaches the semi-sphere focus, the position of the monopole g_1 goes to $z = -\infty$, and the magnetic field changes its sign, which is determined by the sign of the monopole. So at this point there is a reversion in the magnetic monopole, and in the line of magnetic charge, since its sign must be opposite than that of the monopole.

There are still some opened questions about this problem. The main may be the lack of an expression for the magnetic charges of the monopoles and also for the lines of magnetic charges. But further, one may have noticed that we did not propose an image charges configuration for the case in which $z_0 > 0$. Obviously the monopole is not located at R^2/z_0 , since this is in the same region as the real electric charge. Due to the symmetry of the problem, one possible configuration would be the monopole located at $-R^2/z_0$ for $0 < z_0 < R$, and at $-z_0$ for $R < z_0$.

As a last remark, all the calculations were made considering only the first order contribution to the electric field, so the full treatment requires to consider also the electric response of the topological insulator. In this scenario, besides the image monopoles one must find image electric charges that, together with the magnetic monopoles, exhibit dyon's properties [26]. Solutions for electric responses of insulators in this geometry were not found in literature.

4.4 Appendix

To obtain the magnetic field along the z axis, we must use the current given by Eq. (4.1) in the Biot-Savart law [41]:

$$\mathbf{B}(z\hat{\mathbf{z}}) = \frac{1}{c} \int_{\mathcal{S}} \frac{\mathbf{J}_{Hall}(\mathbf{r}') \times (z\hat{\mathbf{z}} - \mathbf{r}')}{|z\hat{\mathbf{z}} - \mathbf{r}'|^3} da',$$

where \mathcal{S} is the semi-spherical interface, da' is the infinitesimal area element and c is the speed of light. Developing this, we are lead to:

$$\mathbf{B}(z\hat{\mathbf{z}}) = -2\pi \frac{e^2}{2h} \frac{qz_0}{c} R^3 \hat{\mathbf{z}} \left\{ \int_{\frac{\pi}{2}}^{\pi} \frac{\sin \theta}{(a + b \cos \theta + d \cos^2 \theta)^{\frac{3}{2}}} d\theta - \int_{\frac{\pi}{2}}^{\pi} \frac{\sin \theta \cos^2 \theta}{(a + b \cos \theta + d \cos^2 \theta)^{\frac{3}{2}}} d\theta \right\},$$

being $a = (R^2 + z_0^2)(R^2 + z^2)$, $b = -2R(zR^2 + zz_0^2 + z_0R^2 + z_0z^2)$, and $d = 4R^2zz_0$

The first integral can be easily solved analytically, but to the second one it is very useful to resort to Eq. (2.264-7) from Ref. [44]. The final expression is:

$$\frac{\mathbf{B}(z\hat{\mathbf{z}})}{2\pi \frac{e^2}{2h} \frac{qz_0}{c} R^3} = -\hat{\mathbf{z}} \left\{ \begin{array}{l} \frac{4d - 2b}{(4ad - b^2)\sqrt{a - b + d}} + \frac{2b}{(4ad - b^2)\sqrt{a}} + \\ \quad + \frac{1}{d(4ad - b^2)} \left[\frac{4ad - 2b^2 + 2ab}{\sqrt{a - b + d}} - \frac{2ab}{\sqrt{a}} \right] + \\ \quad + \frac{1}{d\sqrt{d}} \ln \frac{2\sqrt{d(a - b + d)} - 2d + b}{2\sqrt{ad} + b} \quad \text{if } zz_0 > 0 \\ \\ \frac{4d - 2b}{(4ad - b^2)\sqrt{a - b + d}} + \frac{2b}{(4ad - b^2)\sqrt{a}} + \\ \quad + \frac{1}{d(4ad - b^2)} \left[\frac{4ad - 2b^2 + 2ab}{\sqrt{a - b + d}} - \frac{2ab}{\sqrt{a}} \right] + \\ \quad + \frac{1}{d\sqrt{-d}} \left[\arcsin \frac{b}{\sqrt{b^2 - 4ad}} - \arcsin \frac{b - 2d}{\sqrt{b^2 - 4ad}} \right] \quad \text{if } zz_0 < 0 \end{array} \right.$$

Bibliography

- [1] J. M. Fonseca, “*Algumas contribuições ao estudo do grafeno e dos isolantes topológicos*”, Tese de doutorado, Departamento de Física, Universidade Federal de Viçosa, (2012), disponível em http://www.tede.ufv.br/tedesimplificado/tde_arquivos/49/TDE-2012-03-26T093222Z-3651/Publico/texto%20completo.pdf.
- [2] P. Coleman, “*Introduction to many-body physics*”, Cambridge University Press, New Jersey, (2015).
- [3] P. Phillips, “*Advanced solid state physics*”, Westview Press, Boulder, (2003).
- [4] K. v. Klitzing, G. Dorda, M. Pepper, “*New method for high-accuracy determination of the fine-structure constant based on quantized hall resistance*”, Physical Review Letters, **45**, 494 (1980).
- [5] J. E. Avron, D. Osadchy, R. Seiler, “*A Topological Look at the Quantum Hall Effect*”, Physics Today, **56(8)**, 38-42 (2003).
- [6] M. Z. Hasan, C. L. Kane, “*Colloquium: Topological insulators*”, Rev. Mod. Phys. **82**, 3045-3067 (2010).
- [7] C. Kane and J. Moore, “*Topological insulators*”, Physics World, february, 32 (2011).
- [8] X.-L. Qi, S.-C. Zhang, “*The quantum spin Hall effect and topological insulators*”, Physics Today, **63(1)**, 33-38 (2010).
- [9] J. M. Fonseca, W. A. Moura-Melo, and A. R. Pereira, “*Geometrically induced electric polarization in conical topological insulators*”, Journal of Applied Physics, **111**, 064913 (2012).
- [10] J.E. Moore, “*The birth of topological insulators*”, Nature, **464**, 194 (2010).

- [11] B. A. Bernevig, T. L. Hughes, and S.-C. Zhang, “*Quantum Spin Hall Effect and Topological Phase Transition in HgTe Quantum Wells*”, Science , **314**, 1757 (2006).
- [12] M. König, S. Wiedmann, C. Brüne, A. Roth, H. Buhmann, L. W. Molenkamp, X.-L. Qi and S.-C. Zhang “*Quantum Spin Hall Insulator State in HgTe Quantum Wells*”, Science, **318**, 766 (2007).
- [13] X.-L. Qi and S.-C. Zhang, “*Topological insulators and superconductors*”, Rev. Mod. Phys. **83**, 1057-1110 (2011).
- [14] W. P. Su, J. R. Schrieffer and A. J. Heeger, “*Solitons in Polyacetylene*”, Physical Review Letters, **42**, 1698 (1979).
- [15] X.-L. Qi, T. L. Hughes and S.-C. Zhang, “*Fractional charge and quantized current in the quantum spin Hall state*”, Nature physics, **4**, 273-276 (2008).
- [16] J. Goldstone and F. Wilczek, “*Fractional Quantum Numbers on Solitons*”, Physical Review Letters, **47**, 986 (1981).
- [17] Y. Ran, A. Vishwanath, and D.-H. Lee, “*Spin-Charge Separated Solitons in a Topological Band Insulator*” Physical Review Letters, **101**, 086801 (2008).
- [18] X.-L. Qi and S.-C. Zhang, “*Spin-Charge Separation in the Quantum Spin Hall State*”, Physical Review Letters, **101**, 086802 (2008).
- [19] L. Fu, C. L. Kane, and E. J. Mele, “*Topological Insulators in Three Dimensions*”, Physical Review Letters, **98**, 106803 (2007).
- [20] J. E. Moore and L. Balents, “*Topological invariants of time-reversal-invariant band structures*”, Physical Review B, **75**, 121306(R) (2007).
- [21] R. Roy, “*Topological phases and the quantum spin Hall effect in three dimensions*”, Physical Review B, **79**, 195322 (2009).
- [22] L. Fu and C. L. Kane, “*Topological insulators with inversion symmetry*”, Physical Review B, **76**, 045302 (2007).
- [23] D. Hisieh, D. Qian, L. Wray, Y. Xia, Y. S. Hor, R. J. Cava and M. Z. Hasan, “*A topological Dirac insulator in a quantum spin Hall phase*”, Nature, **452**, 970-974 (2008).

- [24] X.-L. Qi, T. L. Hughes and S.-C. Zhang, “*Topological field theory of time-reversal invariant insulators*”, Physical Review B, **78**, 195424 (2008).
- [25] L. D. Landau and E. M. Lifshitz, “*Electrodynamics of continuous media*” 2nd ed., Pergamon, Oxford (1984).
- [26] X.-L. Qi, R. Li, J. Zang, S.-C. Zhang, “*Inducing a Magnetic Monopole with Topological Surface States*”, Science, **323**, 1184-1187 (2009).
- [27] S. C. Zhang, T. H. Hansson, and S. Kivelson, “*Effective-Field-Theory Model for the Fractional Quantum Hall Effect*”, Physical Review Letters, **62**, 82 (1989).
- [28] J. M. Fonseca, W. A. Moura-Melo and A. R. Pereira, “*Geometrically induced electric polarization in conical topological insulators*”, Journal of Applied Physics, **111**(6), 064913 (2012).
- [29] A. Karch, “*Electric-Magnetic Duality and Topological Insulators*”, Physical Review Letters, **103**, 171601 (2009).
- [30] J. Maciejko, X.-L. Qi, H. D. Drew and S.-C. Zhang, “*Topological Quantization in Units of the Fine Structure Constant*”, Physical Review Letters, **105**, 166803 (2010).
- [31] W.-K. Tse and A. H. MacDonald, “*Giant Magneto-Optical Kerr Effect and Universal Faraday Effect in Thin-Film Topological Insulators*”, Physical Review Letters, **105**, 057401 (2010).
- [32] L. Ohnouteck, M. Hakl, M. Veis, et al. “*Strong interband Faraday rotation in 3D topological insulator Bi₂Se₃*.”, Scientific reports, **6**, (2016).
- [33] V. Dziom, A. Shuvaev, A. Pimenov, G. V. Astakhov, C. Ames, K. Bendias, J. Böttcher, G. Tkachov, E. M. Hankiewicz, C. Brüne, H. Buhmann, and L. W. Molenkamp, “*Observation of the universal magnetoelectric effect in a 3D topological insulator*”, arXiv:1603.05482v1 (2016).
- [34] K. N. Okada, Y. Takahashi, M. Mogi, R. Yoshimi, A. Tsukazaki, K. S. Takahashi, N. Ogawa, M. Kawasaki and Y. Tokura, “*Observation of topological Faraday and Kerr rotations in quantum anomalous Hall state by terahertz magneto-optics*”, arXiv:1603.02113 (2016)

- [35] P. Curie, “*Sur la possibilité d’existence de la conductibilité magnétique et du magnétisme libre (On the possible existence of magnetic conductivity and free magnetism)*”, Séances de la Société Française de Physique, p76 (1894).
- [36] P.A.M. Dirac, “*Quantised singularities in the electromagnetic field.*”, Proceedings of the Royal Society of London A: Mathematical, Physical and Engineering Sciences, **133**, 821, The Royal Society, 1931.
- [37] Wen, Xiao-Gang, and E. Witten. “*Electric and magnetic charges in superstring models.*”, Nuclear Physics B **261**, 651-677 (1985).
- [38] C. Castelnovo, R. Moessner and S. L. Sondhi, “*Magnetic monopoles in spin ice*”, Nature **451**, 42 (2007).
- [39] L. A. S. Mol, R. L. Silva, R. C. Silva, A. R. Pereira, W. A. Moura-Melo and B. V. Costa, “*Magnetic monopole and string excitations in two-dimensional spin ice*”, J. Appl. Phys. **106**, 063913 (2009).
- [40] L. A. S. Mol, W. A. Moura-Melo and A. R. Pereira, “*Conditions for free magnetic monopoles in nanoscale square arrays of dipolar spin ice*”, Phys. Rev. B, **82**, 054434 (2010).
- [41] J. D. Jackson, “*Classical Electrodynamics*”, John Wiley, New York, (1999).
- [42] E. Witten, “*Dyons of charge $e\theta/2\pi$* ”, Physics Letters B, **86**, 283 (1979).
- [43] A. Béché, R. V. Boxem, G. V. Tendeloo and J. Verbeeck, “*Magnetic monopole field exposed by electrons*”, Nat. Phys. **10**, 26-29 (2014).
- [44] I. S. Gradshteyn and I. M. Ryzhik, “*Table of Integrals, Series, and Products*”, Academic Press, NewYork, (2007).